Some imaging strategies in multi-angle spatial compounding

Wilhjelm, Jens E.; Jensen, M. S.; Brandt, T.; Sahl, B.; Martinsen, Kjeld; Jespersen, Søren Kragh; Falk, E.

Published in:
Proc. IEEE Ultrasonics Symposium 2000

Link to article, DOI:
10.1109/ULTSYM.2000.921633

Publication date:
2000

Document Version
Publisher's PDF, also known as Version of record

Some Imaging Strategies in Multi-Angle Spatial Compounding

J. E. Wilhjelm[1], M. S. Jensen[1], T. Brandt[1], B. Sahl[3], K. Martinsen[1], S. K. Jespersen[2] and E. Falk[3]

Center for Arteriosclerosis Detection with Ultrasound (CADUS)
E-mail: wilhjelm@it.dtu.dk. Homepage: www.it.dtu.dk/~wilhjelm/cadus
[1]Dept. of Information Tech., Tech. University of Denmark, Bldg. 344, DK-2800 Lyngby, Denmark.
[2]Novo Nordisk A/S, Brennum Park, DK-3400 Hillerød, Denmark,
[3]Dept. of Exp. Clinical Research, Skejby University Hospital, Århus, Denmark

ABSTRACT

Multi-angle compound images were generated with four schemes: mean, median, root-mean-square and geometric mean. The in vitro images, based on formalin fixed porcine tissue, were analyzed by visual inspection and by calculation of speckle contrast and contrast between different tissues. The mean and rms images featured the largest enhancement of distributed specular reflections. The median image appears somewhat noisy. However, the quantitative analysis did not indicate large differences between the images.

1 . Introduction

Multi-Angle Compound Imaging (MACI) offers potentials for image improvements, due to the reduced angle-dependence and the reduced speckle in the ultrasound image compared to conventional B-mode imaging.[2, 3, 1]. With MACI, images are recorded from a number of different angles, and these single-angle images are then combined to form the final image. In previous investigations, the single-angle images have typically been *averaged* to form the MACI image. This paper reports on four alternative strategies.

2 . Biological Materials

An approximately 40 mm long piece of porcine fatty muscle was formalin fixed while folded along an 8 mm metal rod, to have the fixed muscle somewhat mimic part of a sclerotic vessel wall. After 24 hours of fixation, the tissue was placed - supported by two wires - in a mold, and degassed liquid agar (1 $\%_{\text{weight}}$ agar-agar) was slowly poured into the mold. When filled, a lit with rows of rectangular openings was placed on top of the liquid agar. When set, the agar block contained two rows of index markers on the top, that both could be recognized by ultrasound and later by the operator, who sliced the agar block.

3 . Experimental Scanning System

The experimental system consisted of 1) a MACI (off-line) ultrasound scanner (denoted the Xtra system) developed at our laboratory and previously described,[3] 2) a 192-element 7.5 MHz linear array transducer 40 mm wide[3], 3) a tank with degassed demineralized water at ~20°C into which the agar block was submerged, 4) a 3D translation system capable of manipulating the transducer and finally 5) a control computer. The transducer geometry and center frequency was specifically optimized for scanning the carotid artery.

In order to automatically record data from a number of parallel scan planes, the control computer was connected via an RS232 interface to the 3D translation system as well as to the Xtra system. Thus the Xtra system could remotely record a set of single-angle images and store these on disk. Data was saved as raw radio frequency beamformed signals (12 bits resolution).

The Time-Gain Compensation (TGC) applied to each individual received signal was 10 dB per cm depth. The tissue was scanned in water and agar, so after recording this TGC was removed and substituted with a TGC that only increased inside the tissue region. The slope was here 12.3 dB per cm depth.

4 . Scanning and Slicing Procedure

The agar block with the porcine tissue was placed in the scanning tank and 65 cross-sectional images inter-spaced 0.5 mm were recorded for the angles: $\theta \in [-21°, -14°, -7°, 0°, 7°, 14°, 21°]$. The recorded rf

0-7803-6365-5/00/$10.00

data were scan converted to form raw single-angle images, $I(z, x, \theta; y)$ associated with angle θ and cross-sectional scan plane y. z and x constitute the image plane. The fully compounded region is a triangle[3] and the majority of the tissue specimen was inside this triangular region.

During the subsequent slicing, macroscopic photos were taken of each slice. The tissue slices were subsequently analyzed histologically. Twelve slices were cut and the associated ultrasonic image for each slice was identified by means of the index markers on the top of the agar block.

5 . Compound Image Formation

The "conventional" MACI image is formed by averaging the single-angle images over all angles

$$I_{MACI}(z,x;y) = \underset{\theta}{\text{mean}}\{I(z,x,\theta;y)\} \quad (1)$$

An alternative estimate of the mean is obtained by using the median:

$$I_{med}(z,x;y) = \underset{\theta}{\text{median}}\{I(z,x,\theta;y)\} \quad (2)$$

An approach that weights the individual values differently, depending on their value, can be realized by using the root-mean-square (rms) value:

$$I_{rms}(z,x;y) = \sqrt{\underset{\theta}{\text{mean}}\{I(z,x,\theta;y)^2\}} \quad (3)$$

Finally, from an implementation point of view, it is relevant to consider the averaging process in (1) done *after* the logarithmization. The resulting image in dB will be $\text{mean}_\theta\{20\log_{10}(I(z,x,\theta; y)\}$. After re-arranging, the image before log-compression is then the geometric mean:

$$I_\Pi(z,x;y) = \left[\prod_\theta I(z,x,\theta;y)\right]^{1/N_\theta} \quad (4)$$

where N_θ is the number of single-angle images.

6 . Image Analysis

Two quantitative measures that would be desirable to maximize when imaging tissue with different components are *i)* the signal-to-noise at a point[4], SNR_0, (inverse of speckle contrast) within a region of the same material and *ii)* the contrast between regions of different materials. A high SNR_0 corresponds to a low degree of speckle and thereby a smooth appearance. The higher the contrast the easier tissues can be distinguished. The four types of strategies defined in (1) to (4) were evaluated with these two parameters.

SNR_0 was calculated for the regions with muscle fibre orientation larger than 70° (same definition of this angle as the scan angles), and for the regions with lipid. Thus, the regions with fibres orientated in the interval 0° to 70° were not included in the analysis because the backscattered energy from this angular range features a rather large variation. Specifically, SNR_0 was calculated as the mean of the pixel values in the region, μ, divided by the standard deviation, σ, of the pixel values in the region. Theoretically, for fully developed speckle (*i.e.* pixel values follows a Rayleigh distribution) in a single-angle image, μ/σ can reach 1.91. If compounding N_θ independent images, SNR_0 can theoretically reach $1.91\sqrt{N_\theta}$. Contrast was calculated as $(\mu^2_{muscle}-\mu^2_{lipid})/(\mu^2_{muscle}+\mu^2_{lipid})$.

7 . Results

The subsequent ultrasound images are shown for two scan planes: y_1 and y_2. The macroscopic (anatomical) photo of scan plane y_2 is shown in Figure 1. The corresponding histological image is a geometrically distorted and shrunken version of the

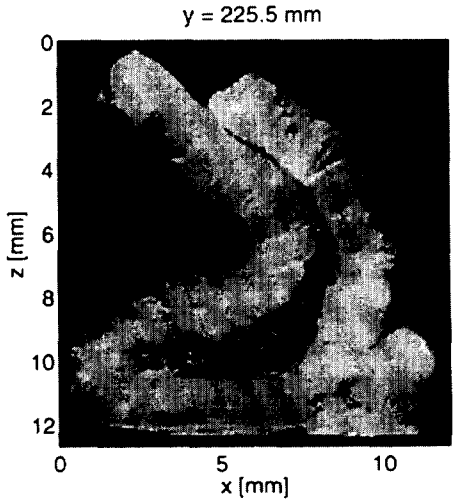

Figure 1 The anatomical image for scan plane y_2.

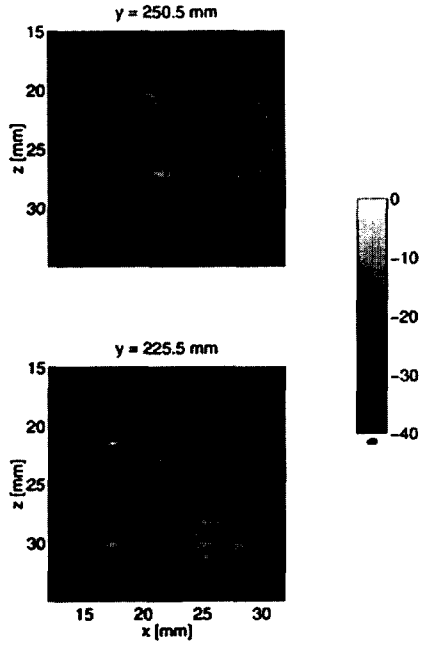

Figure 2 Top: $I_{mean}(z,x;y_1)$. Bottom: $I_{mean}(z,x;y_2)$.

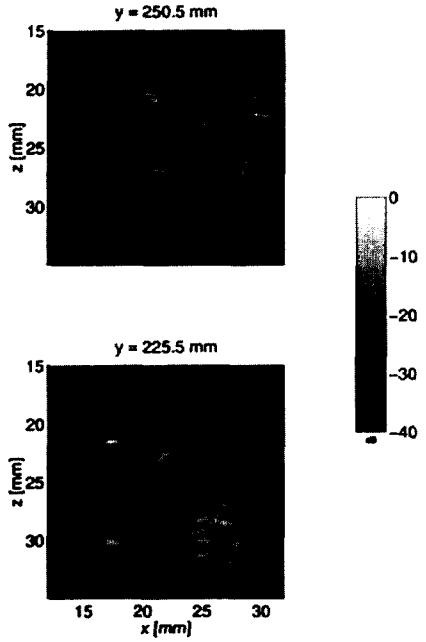

Figure 3 Top: $I_{median}(z,x;y_1)$. Bottom: $I_{median}(z,x;y_2)$.

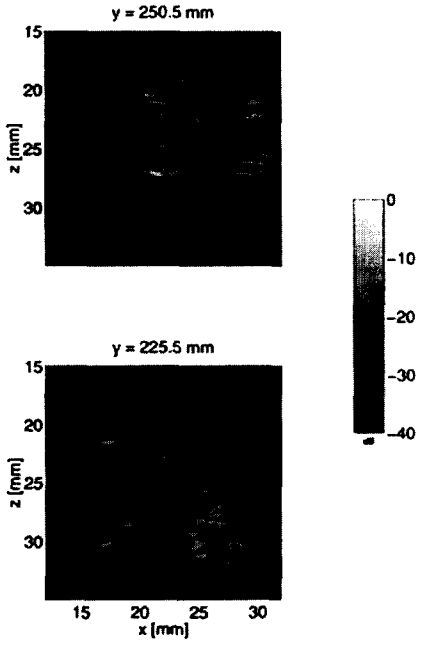

Figure 4 Top: $I_{rms}(z,x;y_1)$. Bottom: $I_{rms}(z,x;y_2)$.

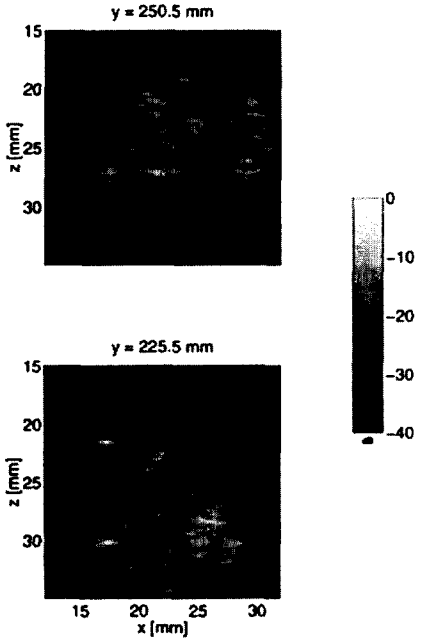

Figure 5 Top: $(I_{\Pi}(z,x;y_1)$. Bottom: $I_{\Pi}(z,x;y_2)$.

macroscopic image due to the histological preparation process. Therefore, both the anatomical and the histological images were used to identify and outline regions of muscle fibres (orientated with angles larger than 70°) and lipid.

Figure 2 shows the "conventional" multi-angle compound images, $I_{mean}(z, x; y)$. All ultrasound images are displayed in dB and the coordinate system have (0,0) in the center of the leftmost transducer crystal. Note that the geometrical shape of the image in Figure

2 does not exactly match that of the anatomical image due to the cutting process. Figures 3 and 4 shows the median and rms images, respectively. Finally, Figure 5 shows the images for the two scan planes, when the geometric mean is used. Each figure uses an individual dB scale.

The relative improvement for the four different compound techniques relative to the 0° image (*i.e.* the conventional B-mode image) is shown in Table 1. The data in the 'SNR_0 simulation' column in Table 1 are calculated the same way as the two other SNR_0 columns, except that the single-angle ultrasound images are substituted with images consisting of random uncorrelated Rayleigh distributed numbers. This somewhat resembles "fully developed" speckle.

Table 1 Improvement in percent relative to the 0° image. The numbers represent the mean of the improvement over 12 scan planes.

	SNR_0, simulation	SNR_0, muscle	SNR_0, lipid	Contrast muscle/lipid
mean	264	154	139	107
median	202	147	137	117
rms	274	149	132	103
Π	223	158	145	127

8 . Discussion

Visual analysis: Figures 2 - 5 reveal only minor differences. The mean and rms images seem to enhance distributed specular components, *e.g.* $(x, z) \sim$ (26-31, 24) mm. This is less pronounced with the geometric mean image and (not surprisingly) even less so with the median image. Specifically, the median image appears more noisy. On the other hand, it can be observed that the inner agar region in scan plane y_2 seems more correctly represented in the median image, $(x, z) \sim$ (19-21, 32) mm.

Quantitative analysis: The results in Table 1 shows that the four methods performs roughly equally. The SNR_0 seldom reached 1.91 in the single-angle images and the improvement for the mean operator was less than $\sqrt{7} = 2.65$. There are a number of reasons for this:

- The regions analyzed in this study were rather small, making it difficult to obtain statistically stable estimates.
- The regions contained interfaces as well as semi-periodic scattering structures, which are known to change the distribution of the pixel values[4].
- If the slope of the TGC applied to the ultrasound scan lines is a little different from the true attenuation, this also influence the speckle statistics.[4]

Thus, the results in Table 1 cannot be used to favor one strategy over another.

It should be noted that the results in this study depend on the scanner settings, the tissue scanned as well as the scan condition. Thus *in vivo* scanning on different tissues potentially can give different results.

9 . Conclusions

The main difference between the four strategies seems to be in the appearance of the images, where distributed specular components are more pronounced in the mean and the rms images. This is less pronounced in the geometric mean image and especially in the median image.

Acknowledgements

This CADUS project was supported by the Danish Technical and Medical Research Councils. The authors gratefully acknowledge the help by M.Sc. Jon Hansen in providing the recording software.

References

[1] Entrekin R, Jackson P, Jago JR, and Porter BA: Real time spatial compound imaging in breast ultrasound: technology and early clinical experience. Medicamundi, Vol. 43, Issue 3, pp. 35 - 43. September 1999.

[2] Hernandez A, Basset O, Chirossel P, Gimenez G: Spatial Compounding in Ultrasonic Imaging Using an Articulated Scan Arm. Ultrasound in Med. & Biol., Vol. 22, No. 2, pp. 229-238. 1996.

[3] Jespersen SK, Wilhjelm JE, Sillesen H: Multi-Angle Compound Imaging. Ultrasonic Imaging, Vol. 20, pp. 81-102, 1998.

[4] Tuthill, TA, Sperry RH and Parker KJ: Deviations from Rayleigh statistics in ultrasonic speckle. Ultrasonic imaging Vol. 10, 1988. pp. 81-89.